International Journal of Luminescence and Applications (ISSN: 2277-6362)
Vol. 5, No. 1, February 2015. Article ID: 053. pp.54-61.

Dependent of Reaction Time on Cu-Doped ZnO Nanostructures Prepared by Chemical Bath Method

L.F. Koao[1*], B.F. Dejene[1], H.C. Swart[3] and T.E. Motaung[2]

[1]*Department of Physics, University of the Free State (QwaQwa Campus), Private Bag X 13, Phuthaditjhaba, 9866, South Africa*
[2]*CSIR Materials Science and Manufacturing, Polymers and Composites Competence Area, Nonwovens and Composites Research Group, P.O. Box 1124, 4 Gomery Avenue, Summerstrand, Port Elizabeth 6000, South Africa*
[3]*Department of Physics, University of the Free State (Bloemfontein), PO Box 339, Bloemfontein, 9300, South Africa.*

Abstract— *Cu-doped ZnO powders were prepared by chemical bath method varying the reaction time at constant synthesis temperature of 80°C and annealed at room temperature. The effect of reaction time on the thermal stability, structure, morphology, optical and luminescence properties of Cu-doped ZnO nanostructures were investigated. The thermogravimetric analysis (TGA) and differential thermogravimetric (DTGA) analysis showed that the best thermal stability is obtained for the sample synthesized for 15 min. The X-ray diffraction (XRD) patterns of the Cu-doped ZnO nanostructures correspond to the various planes of a single hexagonal ZnO phase. The XRD results show that the* $Zn(OH)_2$ *peaks progressively disappear with increasing the reaction time. An increase in reaction time the XRD peaks changed to the pure hexagonal ZnO structure. The diffraction peaks intensity increasewith an increase in reaction time. The estimated average crystallite sizes calculated using the XRD spectra were found to be42 ± 1 and 50 ± 1 nm for samples synthesized at 5 and 15 minutes respectively. It was observed that the estimated average grain sizes increases with an increase in reaction time. The surface morphology study revealed that the grains are irregular at low reaction time but flower-like at high reaction time. The UV-Vis spectra and the band gap energy showed a red shift with an increase in reaction time. The highest luminescence intensity was found for the Cu-doped samples synthesized at 5 min and further increase in reaction time the was decrease in luminescence intensity.*

Keywords— *Reaction Time, Cu-doped ZnO, thermal stability, surface morphology and Luminescence.*

1. INTRODUCTION

Zinc Oxide (ZnO) is well known as a promising optoelectronic material (e.g. Light emitting diodes, solar cells, UV sensors and biosensors) with a wide band gap of 3.37 eV at room temperature, large exciton binding energy of 60 meV[1-3].ZnO is a material that has been the subject of a considerable number of research studies, mostly on the basis of the unique electrical, optical and magnetic properties of material [4]. This material is knownto have many advantages compared to other semiconductors (e.g. ZnS,ZnSe and GaN) andpossesses excellent chemical stability, nontoxicity, easy growth at low cost, and can be synthesized within a few minutes[5-7].It alsohas a rich familyof nanostructured materials. A reduction in grain size to nanometer scale and a change in morphology results in various interesting properties compared to their bulk properties.

Several methods have been used and developed for the synthesis of ZnO at various reaction times. In many of them, the main objective is to reduce the cost of chemical synthesis, and to produce materials for technological applications. Many researchers have synthesized ZnO at various reaction times using sonochemical method [8], hydrothermal [9-10], sol-gel, combustion method, electrochemical deposition and pulse laser deposition method. But those methods require a lot of time to get final yield, need high reaction and annealing temperatures to get rid of Zn(OH), difficult to operate, accurate gas concentrations, and flow rate. So it is very important to find a simple, low temperature method for the synthesis and annealing of ZnO nanostructures and find the way to control the growth parameters. Compared with the above synthesis processes, the ZnO nanostructures were synthesized using the chemical bath deposition method (CBD). This synthesis method showed some advantages compared with the others such asis a simple, cheap and convenient process to prepare semiconducting materials. CBD is a low temperature technique which uses a solution (almost always aqueous) which produces a crystal size that is often very small and homogeneity and lastly can be utilized industrially. There are several parameters in the CBD method that can be varied such as temperature of the bath, the reaction time [7], pH and concentration of precursors [7].Yang et al prepared Eu^{3+} doped ZnO at various reaction times. It was observed that by varying the reaction time the nanosheets aggregate changed to the cactus-like microspheres assembled with single-crystal nanosheets[11]. Other researchers also

* *Corresponding Author Email: koaolf@qwa.ufs.ac.za*

observed that the needle-like hexagonal rods changed to the flower-like structures with the increase in the reaction time [9]. It has been reported that the reaction time is largely influencing the ZnO nanostructures diameters, longer reaction time leads to larger diameter of nanostructures [8]. Also other researchers found that the morphology of the ZnOnanostructures does not depend on the reaction time[7]. They said this is due to the high molar concentration of zinc acetate. Following their footsteps we have reduced the amount of zinc acetate precursor. In this communication, we report the effect of the reaction time on the thermal stability, structure, morphology, optical and luminescence properties of the Cu-doped ZnO nanostructures synthesized by chemical bath deposition method.

2. EXPERIMENTAL DETAILS.

2.1 Procedure

All the chemicals used for the preparation of the nano-powders were of analytical grade. It includes zinc acetate (Zn $(CH3COO)_2.2H_2O$, copper acetate ($Cu(CH_3COO)_2.2H_2O$, thiourea (NH_2CSNH_2) and ammonia (25% NH_3). During the preparation of the nano-powders, ammonia was used as a complexing agent. The Cu-doped ZnO precursors were prepared by dissolving 0.46 M of zinc acetate and 0.4 mol% of copper acetate together in 200 mLof deionized water. 0.18 M thiourea was dissolved in 200 mL of deionized water and 123.5 mL of ammonia were dissolved in 200 mL of deionized water, separately. Then a magnetic stirrer was used to stir each of the mixtures for overnight at room temperature to ensure homogenous distribution of the solution reagents. The chemical bath solution was prepared as follows: 60 mL of zinc and copper acetate mixture, thiourea and ammonia solutions were mixed. An equal volume ratio (1:1:1) was considered for each solution in the following order: 60 mL quantity of zinc and copper acetate mixture was first added to the beaker which was placed in the water bath, followed by addition of 60 mL of thiourea solution and the mixture was stirred for few 5 seconds, following that, 60 mL of ammonia solution was then added fast in the mixture, while continuously stirring [7]. The beakers were removed from the bath at various reaction time intervals (30s, 5 min, and 15 min). It has been observed that the quantity of final yield or precipitates decreases with an increase in reaction time.Water bath was maintained to be at a constant desired temperature of 80°C. The white precipitates were then formed within 30 s after adding ammonia solution. The precipitates increase with an increases in the molar concentration of zinc acetate. The precipitates were then left overnight and filtered thereafter. The precipitates were later washed with 60 mL of ethanol and secondly with 60 mL of acetone. The obtained precipitates were dried at ambient conditions for 3 days. The powders were then ready to be characterized [7].

2.2 Characterization

Thermal analysis carried out by thermogravimetric analyses (TGA) and differential thermogravimetric analyses were performed in a Perkin-Elmer TGA7 thermogravi- metric analyzer. Three samples of Cu-doped ZnO were weighed masses of range 5–10mg and werestudied between 20 and 600 ºC. The heating rate was10 ºC min^{-1} and thegas (N2–8% H2) with aflow-rate of $120cm^3$ min^{-1}.The crystal structures of the samples were determined with a Bruker AXS Discover diffractometer.Operating at40kV and 40mA, and using CuKα = 1.5406 ° A with a scan step of 0.05º in 2θ and a scan speed of 40/min. The morphology of the prepared nanoparticles were determined with a scanning electron microscopy (SEM) using a Shimadzu model ZU SSX-550 Superscan. For SEM measurements, the probe size was 115 nm, the probe current 0.02 nA, and the accelerating voltage 5.0 keV. The reflectance measurements were carried out in the 200 to 800 nm wavelength range using a Perkin Elmer UV/Vis Lambda 20 Spectrophotometer. The integrating sphere was used for the reflectance measurement by diffusion and reflection method. The powders were not suspended in any liquid media and set in the spectrophotometer by putting the powders into a black plastic cell. The bottom of the cell was fully covered with the powder. Photoluminescence spectroscopy (PL) measurements were done on using a SPEX 1870, 0.5M Spectrometer, equipped with a 325 He-Cd laser as the excitation source.

2. RESULTS AND DISCUSSIONS

3.1 Thermal Analysis

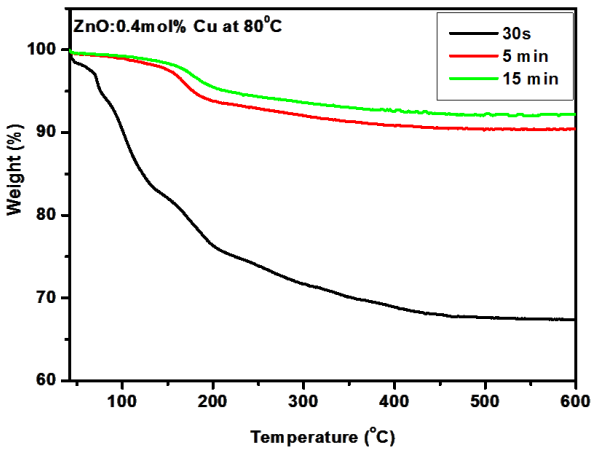

Fig. 1: Thermogravimetric measurements for Cu-doped ZnOnanostructures prepared at different reaction times but at a constant synthesis temperature of 80ºC.

Thermo-gravimetric analysis is a technique by which one can measures the mass loss with respect to the temperature. The thermal behaviors of the Cu-doped ZnOnanopowders synthesized at various reactions times were studied by thermogravimetric analysis (TGA) and differential thermogravimetric measurements (DTGA).

From Fig. 1 and 2 of TGA and DTGA curves it is clear that for Cu-doped ZnOnanopowder synthesized at short reaction time (30s) showed multy (six)degradation steps, meaning several organic materials are degrading or evolving as degree of volatiles. The first step is from 40-91ºC which may be due to the evaporation of ethanol and acetone. The second and major step of weight loss is from 91-147ºC is due to the physically adsorbed water, leaving ZnO and $Zn(OH)_2$ behind.Third step is from 147-228ºC there is decomposition of unreacted acetates ions. Fourth step between 228-304ºC shows the degradation of ammonia. Fifth step which is from 304-366ºC may be due to the relaxation of ZnO skeleton.Sixth step a weight loss was observed from 366-476ºC, indicating the condensation of adjacent hydroxyls and segregated hydroxyls on ZnO surface, in that order. The estimated total weight loss for the sample synthesized at shorter reaction time is 32.5 wt% and it has lower residues.The observed weight loss in the temperature range 200 – 476°C mainly due to phase transformation from $Zn(OH)_2$ to ZnO[12-13]. The Cu-doped ZnOnanopowders synthesized at higher reaction times, 5 and 15 minutes have single step degradationfrom 77-227ºC and 90-247ºC, respectively. The observed weight loss is due to solvent evaporation. The weight loss for Cu-doped ZnOnanopowders synthesized at reaction times of 5 and 15 min is 9.6 and 7.7 wt%, respectively. It is clear that as the reaction time of the CBD increases the amount of organic materials decreases. From the Fig. 1 it is observed that the final residues increase with an increase in reaction times. It can be observed that the best reaction time for preparing ZnOnanopowders using the CBD method is 15 minutes which is highly stable.No further degradation and thermal effect were observed at temperatures in the range of 477 – 600 ºC indicating that a higher temperature is required to conclude a sintering process.

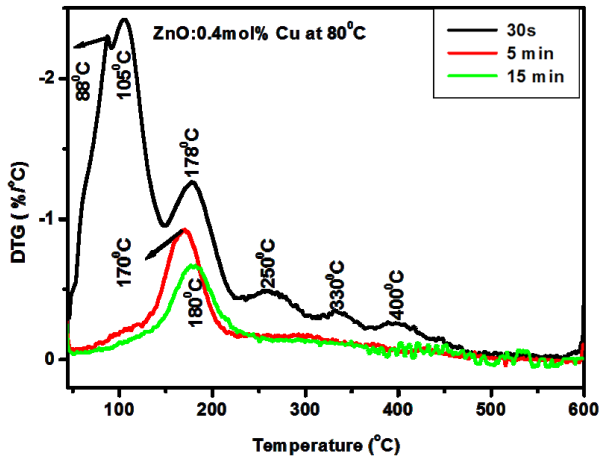

Fig. 2: Differential Thermogravimetric measurements for Cu-doped ZnOnanostructures prepared at different reaction times but at a constant synthesis temperature of 80ºC.

The differential curve ofTG at low reaction time (30s) shows the changes in weight at 88, 105, 178, 250, 330 and 400ºC, respectively. For the Cu-doped ZnOnanopowders synthesized at reaction times of 5 and 15 min the changes in degradation were observed at 170 and 180ºC, respectively. Further heating of the residue to 600ºC did not bring any change in degradation indicating a complete conversion of sample synthesized at reaction time of 30s to a stable phase of ZnO. The zinc atom in sample synthesized at reaction time of 30s is coordinatively saturated by oxygen atoms of acetate and OH ligands, thus eliminating the need of extraneous oxygen to decompose sample synthesized at reaction time of 30s into ZnO.

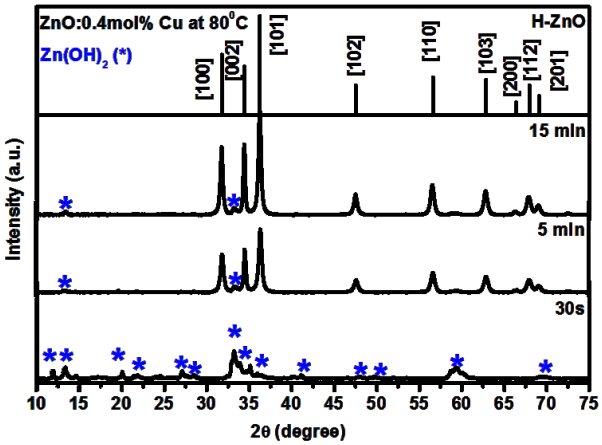

Fig. 3: XRD patterns for Cu-doped ZnO nanostructures prepared at different reaction times but at a constant synthesis temperature of 80ºC.

Figure.3 shows the powder X-ray diffraction patterns of Cu-doped ZnO nanostructures synthesized at various reaction times. The as-synthesized samples at low reaction time (30s) exhibited diffraction peaks corresponding to $Zn(OH)_2$ (*)according to the available powder diffraction JCPDS data of 38-0356 and 3-1464 files, respectively.Terek et al. was able to observe the same behavior of $Zn(OH)_2$ peaks for the as-synthesized ZnO[14]. It was very interesting to note that those $Zn(OH)_2$ peaks diminishes with an increase in annealing temperature [14].From Fig.3 it is clear that by increasing the reaction time the structure of $Zn(OH)_2$ changed to the hexagonal wurtzite structure of ZnOwhich can be indexed to a standard spectrum of JCPDS (No. 36-1451) with the lattice parameters of a= 3.24982 and c =5.20661Å.This behavior of $Zn(OH)_2$ disappearing as the reaction time increases is even observed in TGA analysis. The estimated average lattice parameters using all XRD peaks are a= 3.24316 and c= 5.1986 Å for sample synthesized at reaction time of 5 min and for 15 min are a= 3.25362 and c =5.20997Å. The estimated lattice parameters increase with an increase in reaction time. An increase in lattice parameters confirms that Cu ions are substituted in the Zn sub-lattice generating tensile strain.The average crystallitesizes for the Cu-doped ZnO nanostructures synthesized at various reaction times were estimated

using Scherrer's equation [15]. The estimated average crystallite sizes calculated using the XRD spectra were found to be42 ± 1 and 50 ± 1 nm for samples synthesized at 5 and 15 minutes respectively. It was observed that the estimated average grain sizes increases with an increase in reaction time.The increase in estimated average crystallite sizes is due to the migration of grain boundaries occurs, causing the coalescence of small grains and formation of large grains.

Cu-doped ZnO nanostructures synthesized at reaction times of 5 and 15 min shows diffraction peaks associated with the single phase wurtzite structure of ZnO, although XRD spectrum shows secondary phases assigned to $Zn(OH)_2$. There were no secondary phases due to Cu. This behaviour is due to the XRD peaks shifting toward lower angle as the reaction time increases as shown in Fig. 4. Theshifting is associated to an increase in lattice parameters with an increase in reaction time. This is because of the larger ionic radii of Cu^+ (0.96Å) as compared to that of Zn^{2+} (0.76Å). The shifting of XRD peaks to lower angle indicates that Cu^+ is the main dopant in doped ZnO nanostructures. Because the diameter of Cu^+ is larger than that of Zn^{2+}[16],the doping of Cu^+ in ZnO crystal made the XRD peaks shift to lower angle.Lastly in Fig. 4, the diffraction intensities increase with an increase in reaction time,this indicates an increase in the crystallite size.

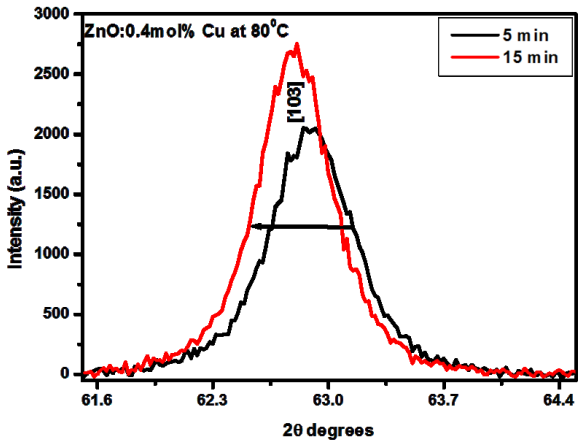

Fig. 4: XRD patterns at (103) Cu-doped ZnO nanostructures prepared at different reaction times but at a constant synthesis temperature of 80°C.

The lattice strain of the synthesized Cu-doped ZnO powders at various reaction times was estimated by a Willamson-Hall plot using the formula[17-18]

$$\beta Cos(\theta) = \frac{K\lambda}{L} + \varepsilon Sin(\theta) \quad (1)$$

whereλ is the X-ray wavelength in nanometer (nm), β is the width of the diffraction peak profile at half maximum height resulting from small crystallite size in radian, L is the crystallite size and K is a constant related to crystallite shape, normally taken as 0.9. The θ can be in degrees or radians, since the cosθ corresponds to the same number and ε is the lattice strain of the Cu-doped ZnO.A model of the Williamson-Hall plot is shown in Fig. 5. The βcosθ value was plotted against sinθ. The θ and β values were taken from the corresponding peaks of X-ray diffraction lines. The strain is equivalent to the slope of the linear fit drawn to the plotted values. The estimated lattice strain are 0.366 ±0.117 and 0.376 ±0.086 for Cu-doped ZnOnanostructures synthesized at various reaction time of 5 and 15 min, respectively. The strain of the nanostructures increases with the increase in reaction time. This firstly may be attributed to the shifting of the diffraction peaks to lower angles and secondly due to the crystallite size that is increasing with the reaction time.

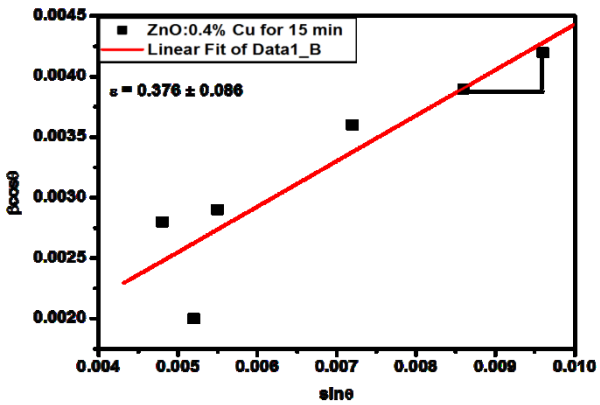

Fig. 5: Williamson-Hall plot showing the linear fit obtained from FWHM for Cu-doped ZnO nanostructures prepared for 15 min but at a constant synthesis temperature of 80°C. The strain was estimated from the slope.

The SEM images of the as-prepared precursors under various reaction times in the CBD process are given in Fig. 6. It can be noticed from figure that the reaction time is an important factor to control the morphology of Cu-doped ZnO structure. At low reaction time (30s) the morphology of sample is irregular and agglomerated as shown in Fig. 6(a). As reaction time is increased to 5 min small irregular particles start to grow into flower-like aggregate in Fig. 6(b). With further increasing the reaction time to 15 minthe morphology is complete changed to theflower-like structure as shown in Fig. 6(c).It is clear that the irregular particles changed to the flower-like structures with an increase in reaction time. The flower-like Cu-doped ZnOnanostructures are clearly consists of cones and they are distributed homogeneous. The morphological data indicate that the structure formation depend of the reaction time.Koao et al. showed that by varying reaction time of the bath there was no effect on morphology [7]. This was due to the use of high zinc acetate molar concentration. Following their paths and reducing the amount of zinc acetate there was a change in morphology.Other researchers showed that by varying the reaction time the needle-like hexagonal rods changed to the flower-like structure [9]. Other group

showed that the crystallites tend to agglomerate as the reaction time increases as shown by SEM [8].Shi et al showed that when the reaction time is about 5 min, a number of nuclei with 60 nm diameters were obtained and dispersed uniformly [19]. Increasing the reaction time the nuclei changed to the flower-like ZnO. Further increasing the reaction time 24 hours makes the diameters of petals more uniform and the flower-like ZnO more defined in the function of the Ostwald ripening mechanism[19]. Polsonkram et al noticed that the shape of the ZnOnanorods are hexagonal and are independent of the deposition time [20]. The nanorod size increases and the density decreases when increasing the deposition time due to the "Ostwald ripening" [20]. The high reaction time of 15 min is therefore sufficient for the synthesis of Cu-doped ZnO nanostructures by CBD.Based on experimental results, it is supposed that ZnO flower-like structures composed of cones. ZnO nanostructures were formed by the following chemical reaction:

$$Zn(CH_3COO)_2 + 2(NH_4)OH \rightarrow Zn(OH)_2 + 2CH_3COONH_4 \quad (2)$$

$$Zn(OH)_2 \rightarrow ZnO + H_2O \quad (3)$$

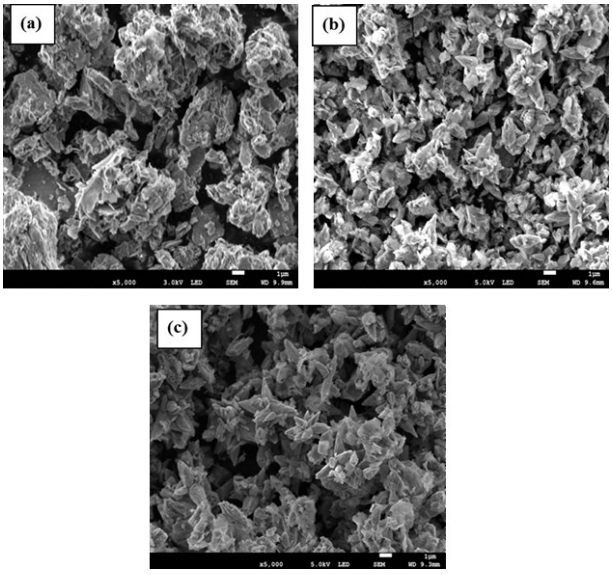

Fig. 6: SEM images for Cu-doped ZnO nanostructures prepared at different reaction times but at a constant synthesis temperature of 80°C.

At the early stage of reaction, ZnO nucleates spontaneously from the solution of $Zn(OH)_2$ to multinuclei aggregates. With the reaction proceeding, these multinuclei aggregates can serve to form flower-like ZnO nanostructures under synthesis temperature of 80°C conditions.

3.2 Optical Properties

3.2.1 Absorption Band

The measurements of diffused reflectance spectrum were preferred over absorption spectra to avoid light scattering effect expected in sample with high aspect ratio of nanostructures. The effect of reaction time on the UV-vis reflectance spectraof the Cu-doped ZnO nanostructures is shown in Fig. 7. Firstly, the Cu-doped ZnO samples show a shift of the absorption edges to higher wavelength with an increase in the reaction time. Secondly, At low reaction time (30s) the absorption edges are not uniform, have many absorption band which are due to $Zn(OH)_2$ as confirmed by TGA and XRD analysis. By further increasing reaction time of the bath the absorption edges become homogeneous with single absorption band of ZnO below 400 nm. The absorption edges below 400 nm are corresponding to the intrinsic band gap of ZnO which is related to electron transitions from the valence band to conduction band. Thirdly the reflectance intensity decrease with an increase in reaction.

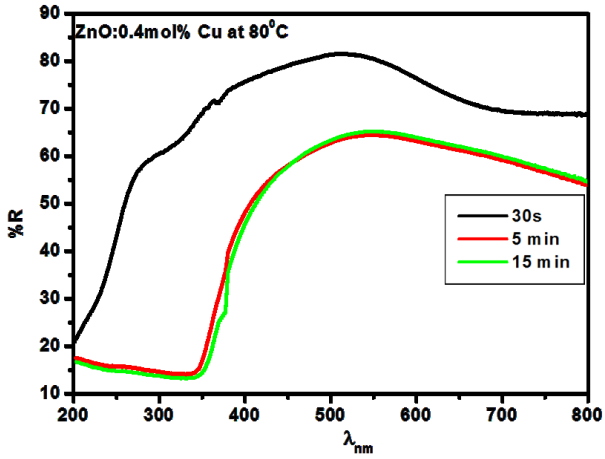

Fig. 7: The reflectance curve for Cu-doped ZnO nanostructures prepared at different reaction times but at a constant synthesis temperature of 80°C.

The band gaps of the Cu-doped ZnO samples were estimated using the Kubelka-Munk remission function [21],

$$K = \frac{(1-R)^2}{2R} \quad (2)$$

Where K is reflectance transformed according to KubelkaMunk, R is reflectancy (%), $h\nu$ is the photon energy. In Fig. 8 the energy band gaps were measured with the help of reflectance spectra plotting graphs of $(K*h\nu)^n$ versus f($h\nu$) [22].E_g is the band gap and n=2 for direct transitions. It can be seen clearly that the band gap energy of the Cu-doped ZnO nanostructures decreases slightly with an increase in the reaction time of the bath. The effect of reaction time is shown in Fig. 8. The estimated band gap energy for the sample synthesized at reaction time of 30s is4.79 ± 0.05, for the Cu-doped ZnO were 3.22 ± 0.01 and 3.21 ± 0.01 eV 5 min and 15min, respectively. All the estimated band gap energies were below the theoretical band gap value of 3.37 eV. Firstly, the red shift of the absorption edges and the reduction of band-gap energy should be due to quantum-size effects.

This may be due to an increase in crystallite size as confirmed by XRD analyses [23]. It is known that as the crystallite size increases, the electronic states are not discrete and results in reducing of the band gap and decreases the oscillator strength[24].Secondly, may be due to the change in morphology as confirmed by SEM analyses.

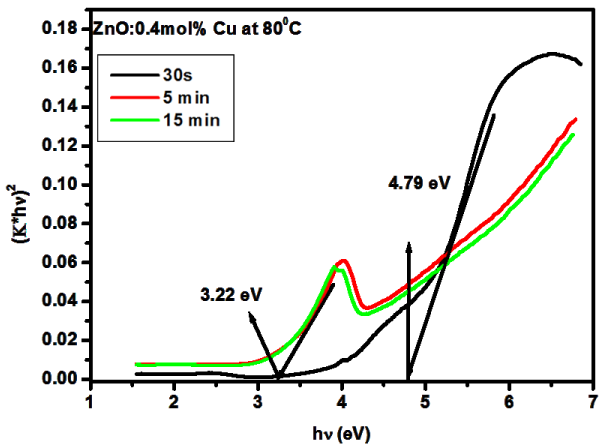

Fig. 8: Plot to determine the band gap energy for Cu-doped ZnO nanostructures prepared at different reaction times but at a constant synthesis temperature of 80°C.

3.3 Photoluminescence Properties

The thermal stability, structural and morphological changes have considerable influence on PL analysis. In order to verify this, the PL analysis was done on Cu-doped samples. Room temperature PL spectrum of prepared samples has been obtained using He-Cd laser having a lasing wavelength of 325 nm as an excitation source. Fig. 9 depicts the PL spectra of $Zn(OH)_2$ nanostructure synthesized at low reaction time of 30s. The PL spectra of Zn(OH)2 nanostructures shows the resolved emission peaks at around 364, 414, 480 and 536 nm. It can be seen from this spectra that the Gaussian curves fitted the PL curves perfectly. Those emission peaks may be attributed to the $Zn(OH)_2$ as confirmed by TGA and XRD analysis.Peng et al observed yellow emission at around 580 nm in the as-prepared sample [25]. However, after annealing treatment, the yellow emission disappears, and meanwhile a green emission peak at around 490 nm occurs, which is commonly thought of the transition related to oxygen vacancy [25]. From Fig. 10 it is observed that by increasing the reaction time those peaks disappear at all. One can easily find two PL peaks for Cu-doped ZnO nanostructures at UV emission around 373 nm corresponding to the near band edge (NBE) emission[26-27]. The UV emission can be explained by NBE transition, namely the free exciton recombination though an exciton-exciton collision process [28-29]. Other broad green emission at around 554 nm that is below the conduction band correspond to the deep level emission (DLE) in ZnO[30], which is related to the intrinsic defects such as O-vacancy (V_0), Zn vacancy (V_{Zn}), O interstials (O_i), Zn interstitial (Zn_i) and extrinsic impurities such as Cu and Li[31].Other researchers suggested that the DLE green luminescence in ZnO indeed is a superposition of different PL bands specifically including Zn-vacancy and O-vacancy related bands [32].

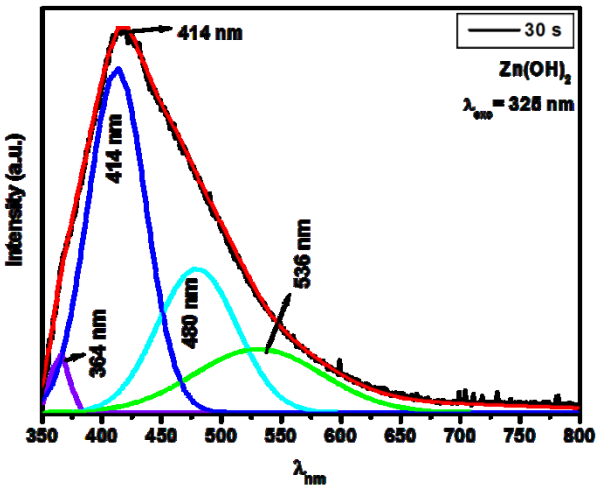

Fig. 9: The Gaussian spectra for Cu-doped Zn(OH)2 nanostructures prepared at reaction timeof 30s.

DLE has been studied by many researchers, but no agreement on its origin has occurred. Other researchers agreed that the green emission is caused by an ionized oxygen vacancy on the surface since it results from the recombination of photo-generated hole with a singly-ionized oxygen vacancy [33]. The stronger the luminescence intensity of the green emission, the more the oxygen vacancies there are [34]. The broad and strong green emission in Fig. 10 indicates that the Cu-doped ZnOnanostructures have a lot of oxygen vacancies [34]. However, the best luminescence intensities in visible region is obtained for Cu-doped ZnO nanostructure synthesized for reaction time of 5 min and further increase in a reaction time there is decreased in luminescence intensities. The increase in luminescence intensity in visible region may be due to the removal of $Zn(OH)_2$ as the reaction time increases as confirmed by TGA and XRD analysis. It is known that the $Zn(OH)_2$ promotes non-radiative recombination.The decrease in luminesce intensities are perhaps due to thetwo reasons: Firstly:to the increase in estimated crystallite as the reaction time increase as confirmed by XRD analysis [7].In other words, their gradual decrease of PL emission intensities reveals a significant decrease in the surface/volume ratio [24]. The PL properties strongly rely on the type and the density of defects in the ZnO nanostructures. The defects in ZnO nanostructures can be trapped and act as recombination centres for charge carriers. If the density of the defects is low, the defects will contribute only to the PL emission resulting in an increase of the luminescence intensity with an increasing density of defects. However, if the density of defects is high, the defects will only behave as the recombination

centres, thus leading to the luminescence intensity decrease with the increase of defect density. Secondly: may be due to the dehydration of $Zn(OH)_2$ during the formation of ZnO when using the CBD method [35]. Lower PL intensities means less recombination rate of photo-induced electrons and holes, and hence more photo-induced carriers could be involved in a nonradiative recombination, whereas higher PL intensity means that more photo induced electrons and holes are recombined.In Fig 10 it is clear that there is shift of luminescence band from 414 nm to 554 nm. This shift may be due to the morphology that is changing with an increase in reaction time as confirmed by SEM analysis.

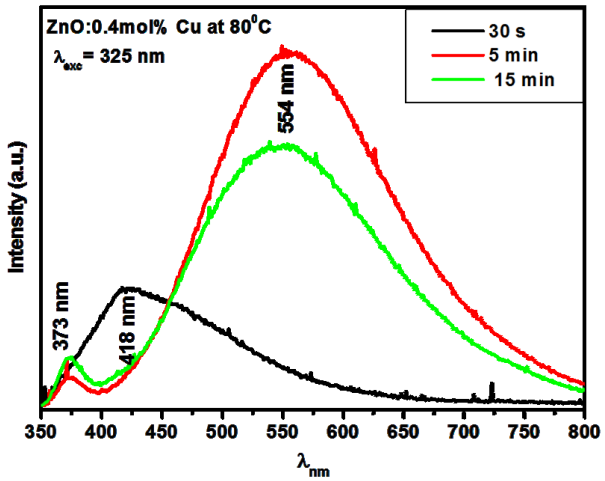

Fig. 10: The photoluminescence spectra for Cu-doped ZnO nanostructures prepared at different reaction times but at a constant synthesis temperature of 80°C.

In UV absorption (373 nm) it is observed that the luminescence intensity increases with an increase in reaction time but there was no shift in luminescence band. This increase in luminescence intensity of the UV with an increase in reaction time is due to. The much higher intensity of the visible peaks compared to that of the UV absorption is an indication of a high density of defects in the crystal of ZnO[8]. Koao et al using the high molar concentration of zinc acetate observed the decrease in luminescence intensity with an increase in synthesis time but with only luminescence band at around 606 nm.The orange band emission was due to the excess oxygen and zinc. Pholnak et al observed that with an increase sonification time there was variation in luminescence intensity only not luminescence band [8]. What is very interesting with this work it can be noticed from TGA,DTGA, XRD, SEM,UV and PL that the reaction time has effect on thermal stability, structure, morphology, optical and luminescence properties. They support each other.

4. CONCLUSION

In summary the Cu-doped ZnO nanostructures were successfully synthesized by CBD method varying the reaction times at bath temperature of 80°C. This method produced a large quantity of Cu-doped ZnO nanostructures at very low cost. The TGA showed that the thermal stability was obtained with an increasing reaction time. The XRD revealed that the average crystallite size of the as-prepared Cu-doped ZnO increased with an increasing reaction time. SEM showed that morphology changed from irregular to the flower-like with increasing reaction time. UVspectroscopy showed the red shift with an increase in reaction time. The PL result showed that the spectra for sample low reaction time the luminescence band is around 414 nm for $Zn(OH)_2$ but with an increase in reaction the Cu-doped ZnO nanostructure shows luminescence peaks at around 373 nm and 543 nm.

ACKNOWLEDGEMENTS

The author would like to acknowledge the National Research Foundation and Department of Science and Technology and the University of the Free State for financial support.

REFERENCES

[1] F.Z. Bedia, A. Bedia, N. Maloufi, M. Aillerie, F. Genty, B. Benyoucef, Journal of Alloys and Compounds,616 (2014) 312-318.

[2] H. Yuan, M. Xu, Q. Z. Huang, Journal of Alloys and Compounds, 616 (2014) 401-407.

[3] R. Wahab, S. G. Ansari, Y. S. Kim, M. A. Dar, H. S. Shin, Journal of Alloys and Compounds, 461 (2008) 66-71.

[4] J. Iqbal, T. Jan, M. Shafiq, A. Arshad, N. Ahmad, S. Badshah, R. Yu, Ceramics International, 40 (2014) 2091-2095.

[5] Ü. Özgür, Y.I. Alivov, C. Liu eta al, Journal of Applied Physics, Article ID 041301, 98(4) (2005) 1-103.

[6] C.F. Klingshirn, ChemPhysChem, 8(6) (2007) 782-803.

[7] L.F. Koao, F.B. Dejene, H.C. Swart, Materials Science in Semiconductor Processing, 27 (2014) 33–40.

[8] C. Pholnak, C. Sirisathitkul, S. Suwanboon, D. J. Harding, Materials Research, 17(2) (2014) 405-411

[9] S. Hussain, T. Liu, M. Kashif, L. Lin, S. Wu, W. Guo, W. Zeng, U. Hashim, Material Science in Semiconductor Processing, 18 (2014) 52-58.

[10] G. Amin, M.H. Asif, A. Zainelabdin, S. Zaman, O. Nur, M. Willander, Journal of Nanomaterial, ID 269692 (2011) 1-9.

[11] J. Yang, X. Li, J. Lang, L. Yang, M. Gao, X. Liu, M. Wei, Y. Liu, R. Wang, Journal of Alloys and Compounds, 509 (2011) 10025-10031.

[12] Y. Khan, S.K. Durrani, M. Mehmood, J. Ahmad, M.R. Khan, S. Firdous, Applied Surface Science, 257 (2010) 1756 - 1761.

[13] W. Jia, S. Dang, H. Liu, Z. Zhang, C. Yu, X. Liu, B. Xu, Materials Letters, 82 (2012) 99 – 101.

[14] T.T. Ali, K. Narasimharao, I.P. Parkin, C. J. Carmalt, S. Sathasivam, S. N. Basahel, S. M. Bawaked, S. A. Al-Thabaiti, Royal Society of Chemistry, DOI:10.1039/c4nj01465k (2014) 1-12

[15] A. Monshi, M. R. Foroughi, M. R. Monshi, World Journal of Nano Science and Engineering, 2 (2012) 154-160.

[16] S. Shen, C. X. Kronawitter, J. Jiang, P. Guo, L. Guo, S. S. A. Mao, Nano Energy, 2 (2013) 958-965.

[17] X. Li, Y. Qu, G. Sun, D. Jiang, X. Ouyang, Journal of Physics and Chemistry of Solids, 68 (2007) 2405-2410.

[18] P. Bindu, S. Thomas, Journal of Theoretical Applied Physics, 8 (2014) 123-134.

[19] R. Shi, P. Yang, X. Dong, Q. Ma, A. Zhang, Applied Surface Science, 264 (2013) 162-170.

[20] D. Polsongkram, P. Chamninok, S. Pukird, L. Chow, O. Lupan, G. Chai, H. Khallaf, S. Park, A. Schulte, Physica B, 403 (2008) 3713-3717.

[21] L.F. Koao, F.B. Dejene, H.C. Swart, J.R. Botha, Journal of Luminescence, 143 (2013) 463-468.

[22] J. Tauc, R. Grigorovici, A. Vancu Sharma, Physica Status Solidi. 15 (1966) 627-629.

[23] M. Farhadi-Khouzani, Z. Fereshteh, M. R. Loghman-Estarki, R. S. Razavi, Journal of Sol-Gel Science and Technology, 64 (2012) 193-199.

[24] S. N. Sahu, K. K. Nanda, ProceedingIndian National Science Academy. 67 (A) (2001) 103-130.

[25] W.Q. Peng, S.C. Qu, G.W. Cong, Z.G. Wang, Material Science in Semiconductor Processing, 9 (2006) 156-159.

[26] X. L. Hu, Y. J. Zhu, S. W. Wang, Materials Chemistry and Physics, 88 (2004) 421-426

[27] Z. Q. Zhu, J. Zhou, International Journal of Minerals, Metallurgy and Materials, 17 (2010) 80-85.

[28] C. Ahn, Y.Y. Kim, D.C. Kim, S.K. Mohanta, H.K. Cho, Journal of AppliedPhysics, 105 (2009) 013502-013502-05.

[29] D.C. Reynolds, D.C. Look, B. Jogai, C.W. Litton, T.C. Collins, W. Harsch, G. Cantwell, PhysicalReview B. 57 (1998) 12151-12155.

[30] M. Willander, O. Nur, J. R. Sadaf, M. I. Qadir, S. Zaman, A. Zainelabdin, N. Bano, I. Hussain, Materials, 3 (2010) 2643-2667.

[31] P. Guo, J. Jiang, S. Shen, L. Guo, International Journal of Hydrogen Energy, 38 (2013) 13097-13103.

[32] P. Klason, T. M. Børseth, Q. X. Zhao, B. G. Svensson, A. Y. Kuznetsov, P. J. Bergman, M. Willander, Solid State Communication, 145 (2008) 321-326.

[33] K. Vanheusden, W. L. Warren, C. H. Seager, D. R. Tallant, J. A. Voigt, B. E. Gnade, Journal ofAppllied Physics, 79 (1996) 7983-7990.

[34] X. X. Yang, W. Lei, X. B. Zhang, B. P. Wang, C. Li, K. Hou, Y. K. Cui, Y. S. Di, Thin Solid Films, 517 (2009) 4385-4389.

[35] C. Florica, N. Preda, M. Enculescu, I. Zgura, M. Socol, I. Enculesc, Nanoscale Research Letters, 385(9) (2014) 1-10.